



Supplement of

The uncertainty of flood frequency analyses in hydrodynamic model simulations

Xudong Zhou et al.

Correspondence to: Xudong Zhou (x.zhou@rainbow.iis.u-tokyo.ac.jp)

The copyright of individual parts of the supplement might differ from the article licence.

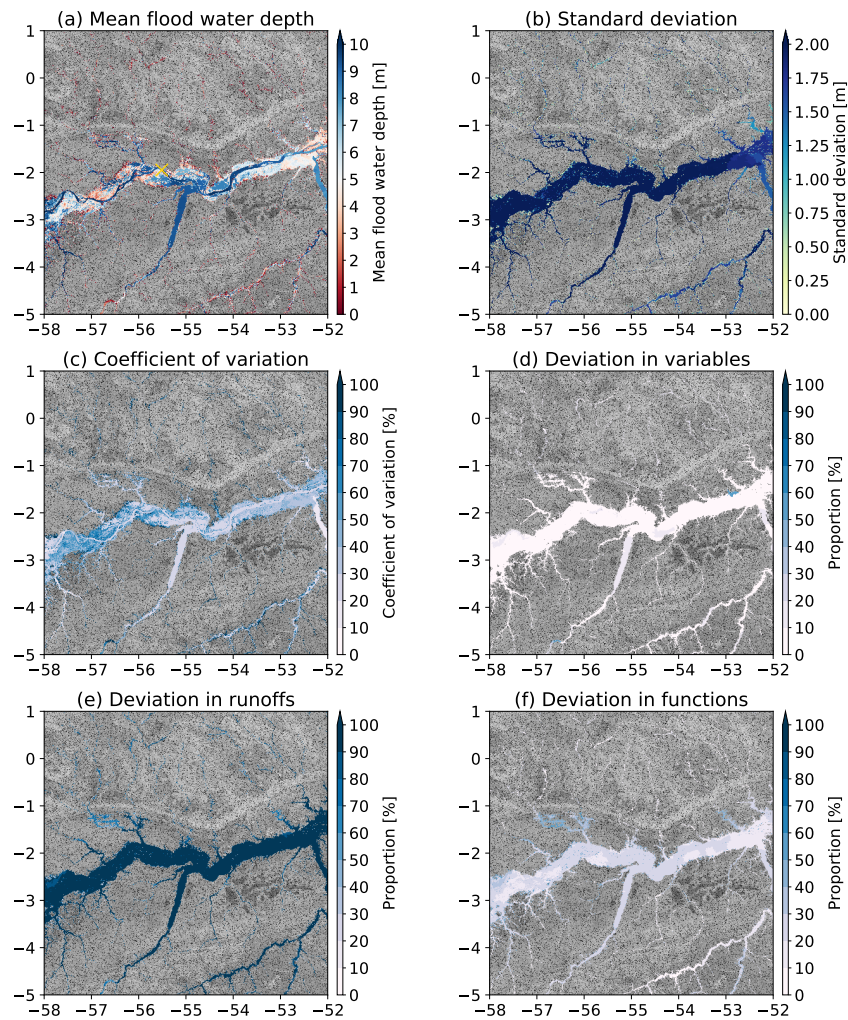


Figure S1. The mean and uncertainties of the flood water depth for 1-in-100 year return period in the lower Amazon River Basin. The mean floodplain water depth (a), the standard deviation (b) and the coefficient of variation (c) are estimated based on all the experiments. The deviation proportion to the overall standard deviation (b) is display in (d)–(f) for different variables, runoffs and fitting functions, respectively. Area with floodplain water depth less than 0.01 m are masked out.

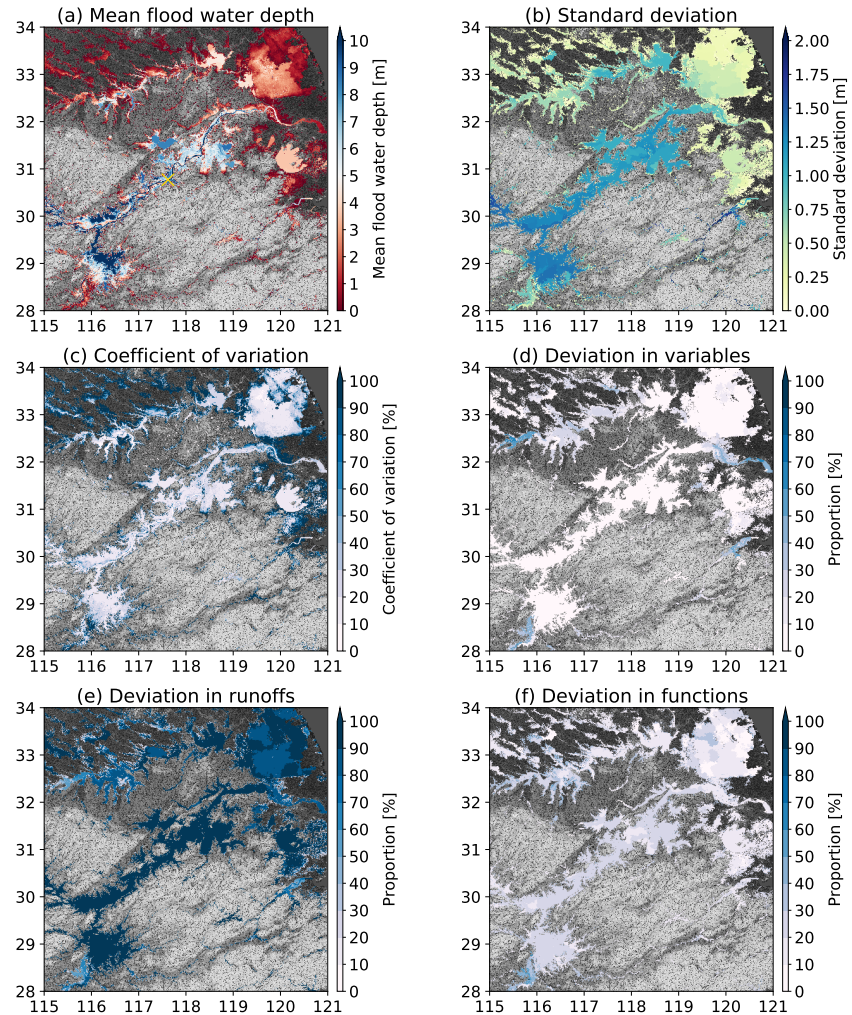


Figure S2. Same as Figure S1, but for lower Yangtze River Basin.

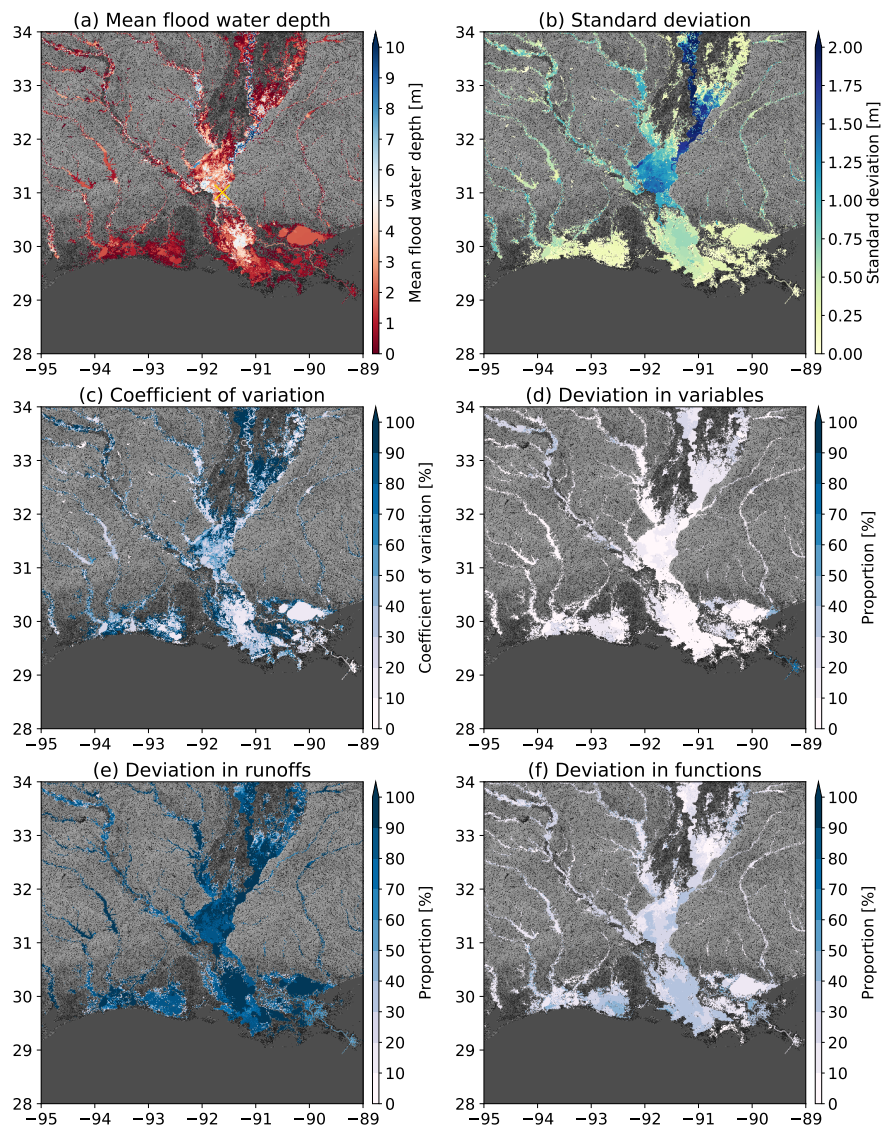


Figure S3. Same as Figure S1, but for lower Mississippi River Basin.

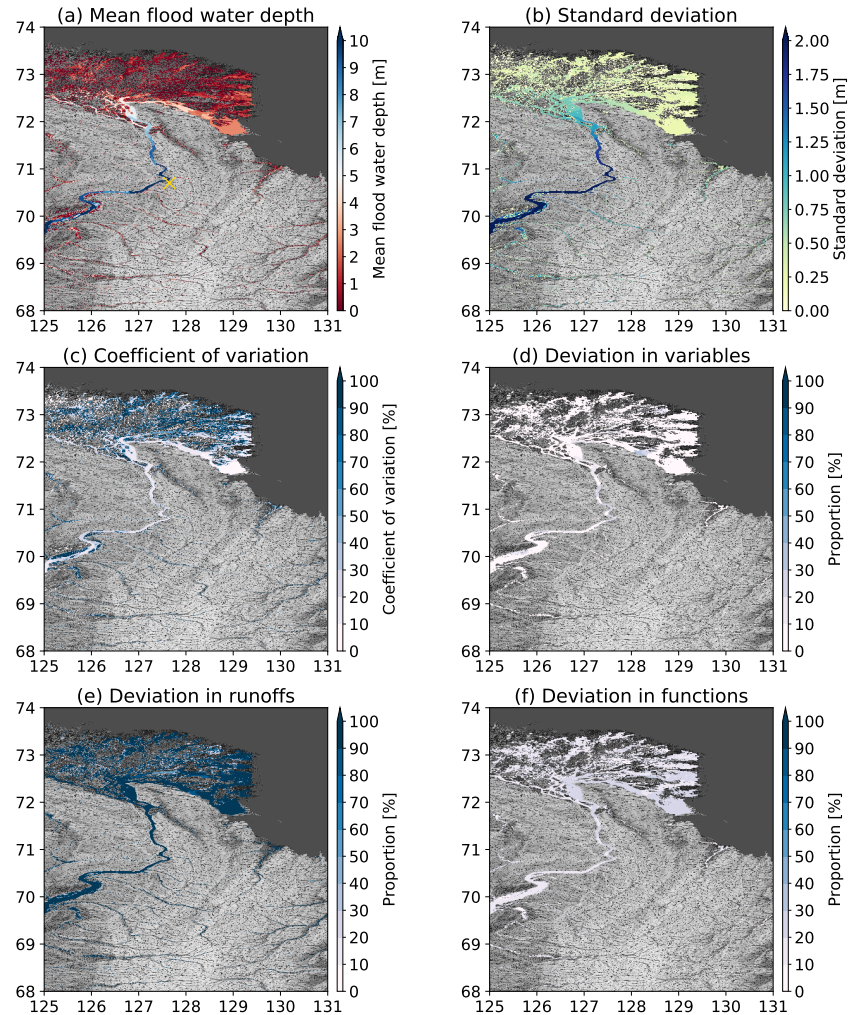


Figure S4. Same as Figure S1, but for lower Lena River Basin.

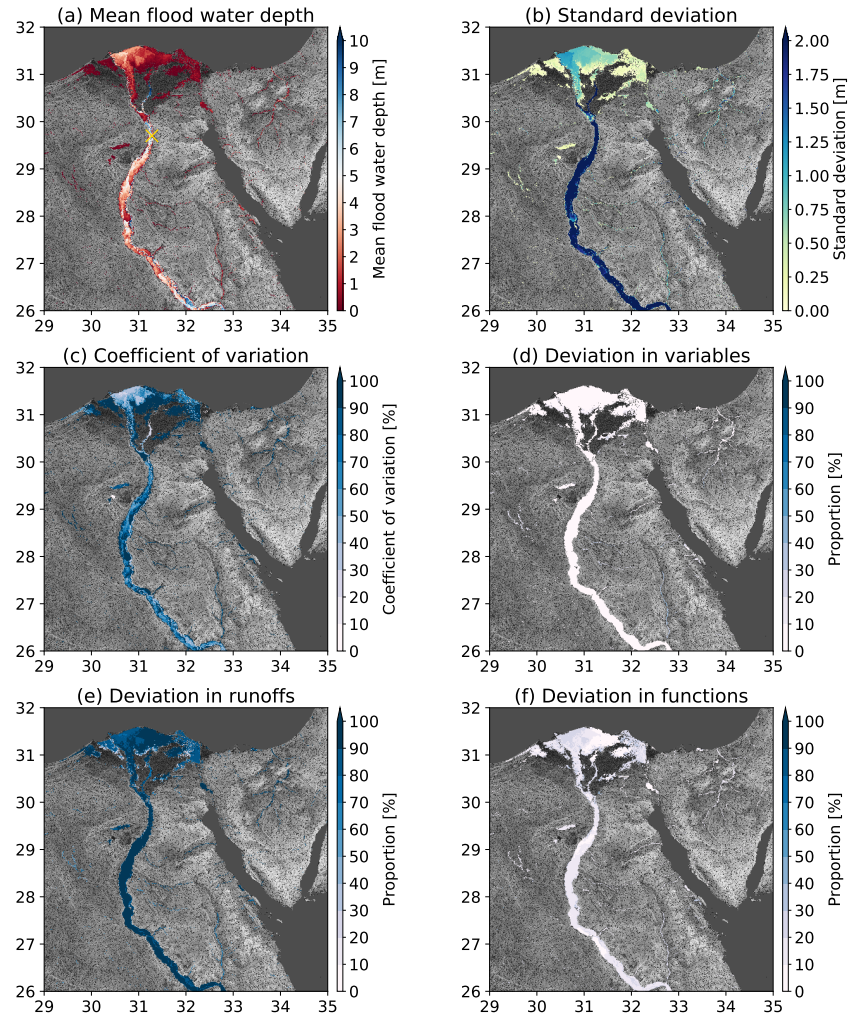


Figure S5. Same as Figure S1, but for lower Nile River Basin.

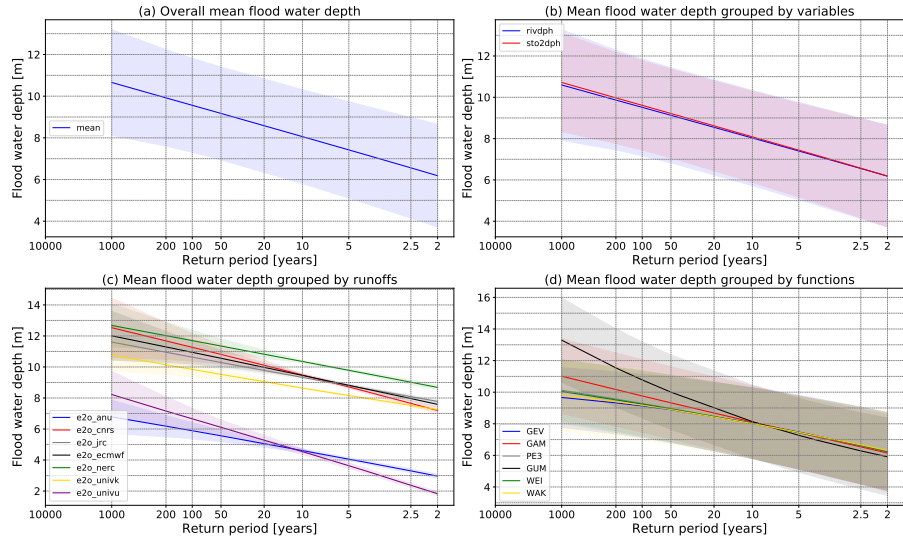


Figure S6. Uncertainties in the estimated floodplain water depth at Obidos (55.5111°W , 1.9472°S) in the Amazon River Basin in different groups. a) the mean floodplain water depth and overall uncertainty; b) the mean and uncertainty in groups of different variables for FFA, the uncertainty is then not related to the selected variable; c) the mean and uncertainty in groups of different runoff inputs, d) the mean and uncertainty in groups of different fitting distributions.

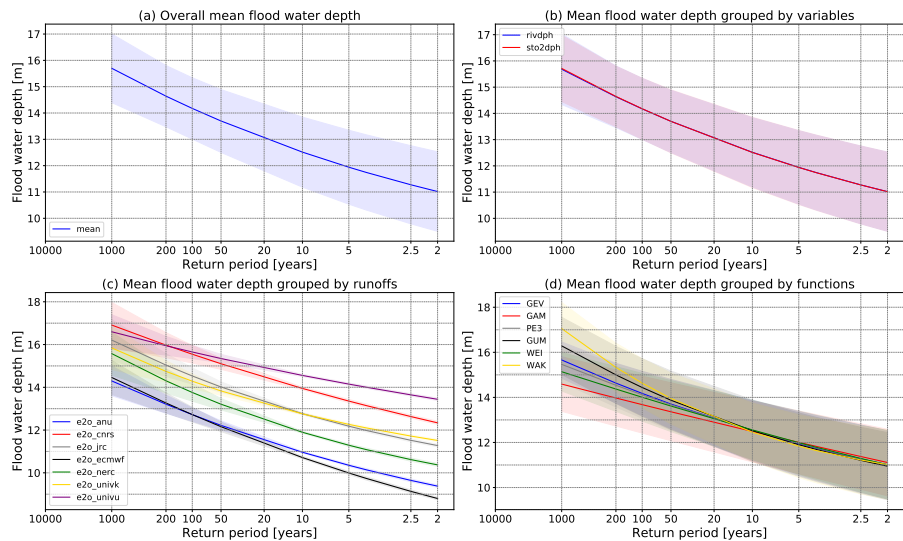


Figure S7. Same as Figure S6, but for the Datong (117.62°E , 30.77°N) in the Yangtze River Basin.

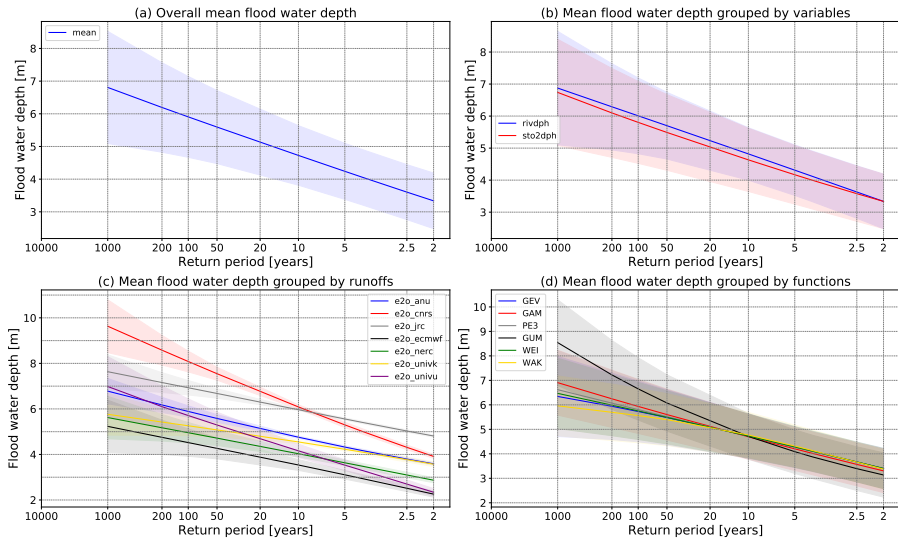


Figure S8. Same as Figure S6, but for the Tarbert Landing (91.6237°W , 31.0085°N) in the Mississippi River Basin.

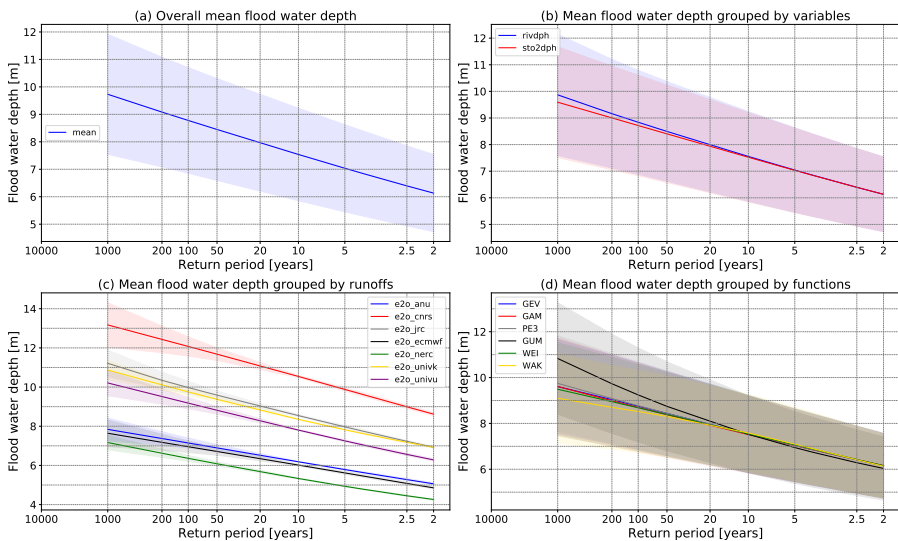


Figure S9. Same as Figure S6, but for the KYUSYUR (KUSUR) (127.65°E , 70.7°N) in the Lena River Basin.

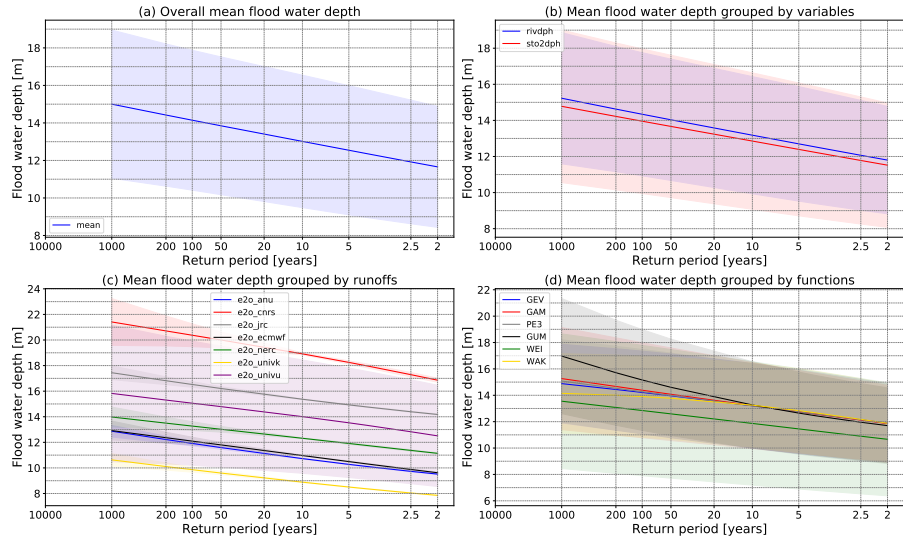


Figure S10. Same as Figure S6, but for the EL EKHSASE (31.28°E , 29.7°N) in the Nile River Basin.

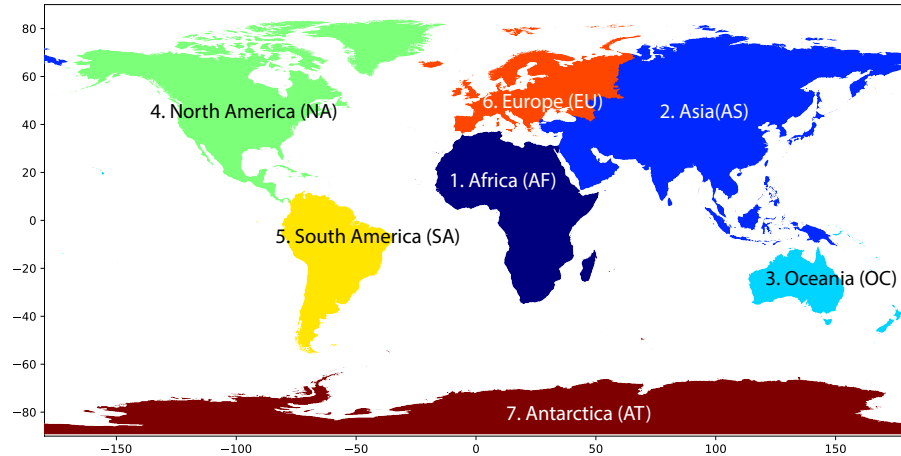


Figure S11. Definition of different continents.

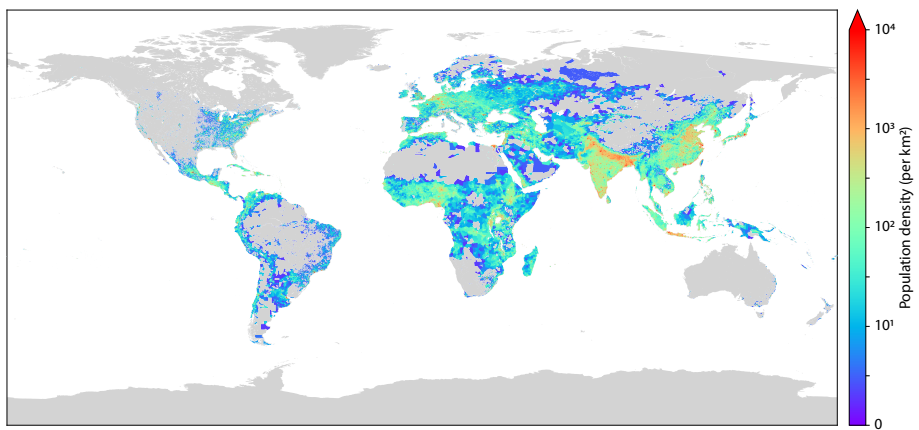


Figure S12. The population density person per km^2 in Gridded Population of the World (GPW v4) for year 2015 (Center for International Earth Science Information Network (CIESIN), 2018).

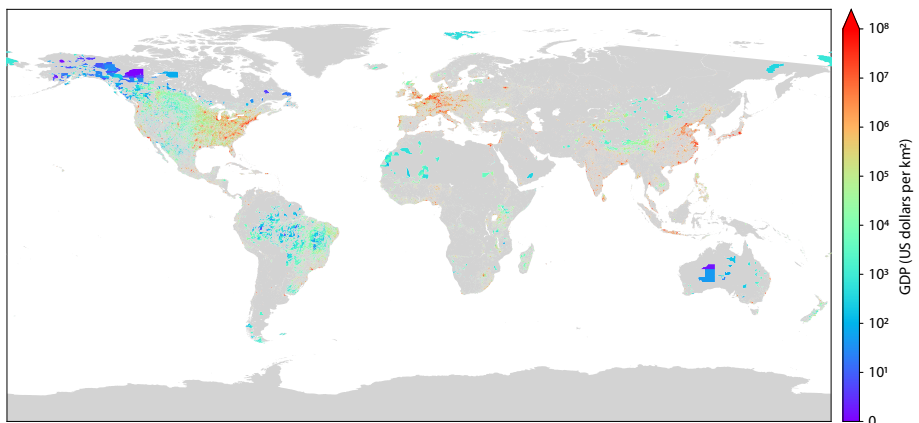


Figure S13. The Gross Domestic Product per km^2 in year 2015 (Kummu et al., 2018).

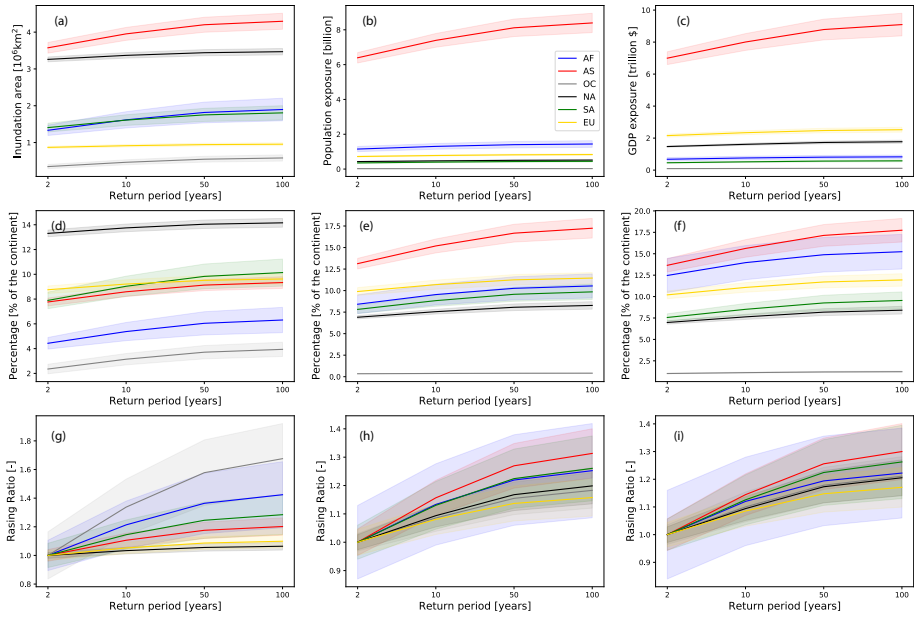


Figure S14. The mean and uncertainties of the inundation area, population exposure and economic exposure for different floods over different continents. The first column is for inundation area; the second is for population and the third is for the GDP in USD. The first row shows the absolute values; the second is the ratio compared to values in specific continents. The third row is normalized value divided by the mean values for 1-in-2 year flood.

References

- Center for International Earth Science Information Network (CIESIN): Documentation for the gridded population of the world, Version 4 (GPWv4), Revision 11 Data Sets, 2018.
- Kummu, M., Taka, M., and Guillaume, J. H.: Gridded global datasets for Gross Domestic Product and Human Development Index over
5 1990-2015, *Scientific Data*, 5, 1–15, <https://doi.org/10.1038/sdata.2018.4>, 2018.